A TEST OF THE EQUIVALENCE PRINCIPLE USING A SPACE BORNE CLOCK

R. F. C. Vessot and M. W. Levine

Center for Astrophysics
Harvard College Observatory and Smithsonian Astrophysical Observatory
Cambridge, Massachusetts 02138

Introduction

On June 18, a Scout D rocket was fired from Wallops Island, Virginia, carrying an atomic hydrogen-maser oscillator system as the payload. The frequency of signals from the oscillator was monitored on the ground at Merritt Island, Florida, by using two hydrogen masers as comparison oscillators. The first-order doppler shift in the signals was eliminated by a go-return transponder link to the payload, and the resulting data, representing the relativistic shifts, were recovered and recorded. The objective of this experiment was to measure directly the effect of the gravitational potential on the frequency of a proper clock, in this case an atomic hydrogen maser.

In the experiment, a gravitational effect amounting to some 4.5 parts in 10^{10} was measured with an oscillator having a stability of about 1 part in 10^{14}. Therefore, to make the best possible use of the oscillator, we must account for all frequency shifts at the 5×10^{-15} level in $\Delta f/f$ in the system, and this, of course, includes all the phase variations that can cause such a shift to appear.

This essay is an outline of the experiment and a preliminary review of the data now available; the data-reduction process is still in progress at this time.

We wish to emphasize that this experiment was conducted by a large number of people and involved many different organizations. The program was managed by the George C. Marshall Space Flight Center (MSFC) of the National Aeronautics and Space Administration (NASA), who were also responsible for designing and assembling the payload structure and testing it before launch. NASA's Goddard Space Flight Center performed the task of tracking and data acquisition, and NASA's Langley Research Center and the Vought Corporation were responsible for the vehicle. The Smithsonian Astrophysical Observatory provided the payload and ground based clocks, the doppler cancelling electronics system and the scientific leadership of the experiment.

$$\frac{\Delta f}{f_0} = \frac{\phi_2 - \phi_3}{c^2} - \frac{|\vec{\beta}_2 - \vec{\beta}_3|^2}{2} - \frac{|\vec{r}_3 - \vec{r}_2|}{c^2}\,\vec{a}_3 \cdot \vec{\epsilon}_{23} \quad . \qquad (1)$$

In this expression, $\phi_2 - \phi_3$ is the Newtonian gravitational potential difference between the probe and the ground station at Merritt Island; $\vec{r}_2$ and $\vec{\beta}_2$ are the position and velocity/c of the probe in an earth-centered inertial frame; $\vec{r}_3$ and $\vec{\beta}_3$ are the position and velocity/c of the ground station in the same frame; $\vec{\epsilon}_{23}$ represents the propagation vector of the probe-to-ground signal; and $\vec{a}_3$ is the centrifugal acceleration of the ground station. Equation (1) contains the expected gravitational shift and the second-order doppler shift, plus a term describing the effect of the earth's rotation during the light time $|\vec{r}_3 - \vec{r}_2|/c$ of the signal from the probe.

The expected behavior of this output signal frequency begins with a value of about -1 Hz near launch (when the gravitational effect is very small and the second-order doppler shift is large), proceeds through a zero beat (when the gravitational and second-order doppler shifts are equal), reaches a rather slowly varying maximum value of about 1 Hz at apogee, and returns through zero beat to about -1 Hz as the probe approaches impact.

Implicit in this experimental test is the assumption that the velocity of light is the same in both directions of propagation to and from the probe. If one a priori assumes that the equivalence principle is valid one can use the results to establish an upper bound on the ratio of the velocity of light in the two directions.

The dependence of the output frequency to an anisotropy of the propagation is given by the following expression (see Appendix A)

$$\frac{\Delta f_c}{f_0} = \frac{\Delta f}{f_0} + \frac{\dot{r}}{2c}\,\frac{\Delta c}{c} \qquad (2)$$

Here $\Delta f/f_0$ is the expected relativistic frequency shift given in equation 1, $\dot{r}$ is the range rate of the probe as seen from the earth station and Δc is the difference in the light velocity in the up and down directions.

Clearly, the phase-coherent system is greatly oversimplified in Figure 5. In practice, different frequencies must be used for each of the three links, and to make

$$\Delta f_{ud} = \frac{40.5}{cf_h} \left(\frac{d}{dt} \int_P \rho \, ds \right) \left(\frac{M}{N} + \frac{N}{M} \right) \frac{1}{2} \frac{S^2}{R^2} \frac{P}{Q} \frac{N}{M} \quad . \tag{3}$$

Similarly, for the oscillator downlink, we get

$$\Delta f_c = \frac{40.5}{cf_h} \left(\frac{d}{dt} \int \rho \, ds \right) \frac{Q}{P} \quad .$$

At the output of the last mixer, the net frequency error is

$$\Delta f_e = \Delta f_c - \Delta f_{ud} = \frac{40.5}{cf_h} \left(\frac{d}{dt} \int_P \rho \, ds \right) \left[\frac{Q}{P} - \frac{S}{2R^2} \left(1 + \frac{N^2}{M^2} \right) \frac{P}{Q} \right] \quad . \tag{4}$$

By selecting the frequency ratios P/Q, N/M, and R/S properly, we can make this error identically equal to zero for all ionospheric variations. Since we had a predetermined transponder ratio, M/N = 240/221, as well as constraints on the usable frequency range in the unified S-band system adapted for the experiment, we chose P/Q = 76/49 and R/S = 82/55. From a typical model of the ionosphere, we find that $\Delta f_c/f$ is, at worst, about 10^{-10} for our experiment. The residual error $\Delta f_e/\Delta f_c$ for this choice of P/Q and M/N is 1.04×10^{-5}, within our experimental error constraint of 5 parts in 10^{15}.

It should be noted here that those ionospheric effects represented by terms of higher order than 1/f are not canceled. In particular, the $1/f^2$ term contains Faraday rotation effects that are nonreciprocal and therefore uncanceled by the system. Terms in $1/f^3$ involve ray-path departures from the assumed straight line given by the path integral in equation (1). Both these terms are being investigated closely from the data near the end of the mission, where the angle of the tracking antenna was 0.4^o above the horizon.

Experiment Operations

The data-acquisition system at Merritt Island recorded the beat frequency in terms of sine and cosine voltages at 14-bit accuracy every 0.01 sec. The beat data were also acquired for "quick-look" purposes by a strip-chart recorder, some features of which are reproduced in Figures 8 through 13.

During the mission, we experienced only one loss of phase coherence, which resulted from a circuit-breaker dropout in the power supply for the uplink transmitter at the Merritt Island station. This problem was quickly solved: Only $1^m 8^s$ elapsed before the probe signals were reacquired, and in less than 50 sec after acquisition, all phase-lock loops were closed and normal data acquisition continued.

A rough approximation of the shape of the beat frequency versus time is given in Figure 14, which is plotted from quick-look frequency measurements.

Experiment Error Sources

The operational data were acquired in the form of digitized sine and cosine voltages that represent the phase of the signals as processed by the doppler-canceling system. These data contained systematic errors from many sources, which, in general, fall into two categories, frequency and phase.

Phenomena that caused frequency changes in either the probe or the ground masers are listed here as frequency errors, while those that produced changes in the phase of the doppler signal are called phase errors. An exhaustive test and calibration program before the launch led to a number of phase and frequency calibrations that are being applied to the predicted frequency effect before comparisons are made with the actual data. These are discussed in the following.

a) Trajectory Determination

The redshift is predicted from our knowledge both of the probe's position and velocity throughout its trajectory and of the earth's geopotential. During the flight, the probe was tracked by three additional unified S-band stations, at Bermuda, Ascension Island, and Greenbelt, Maryland. Each of these stations recorded the doppler frequency of the transponder downlink, which, in turn, was used to generate the probe ephemeris for each second of the flight. Additional data from radar tracking were obtained from the NASA stations in Wallops Island and Bermuda.

From the probe's position and a description of the geopotential, we can predict the redshift at each point in the trajectory. Second-order doppler effects are predicted from the probe's velocity and the known ground-station velocity due to earth rotation. The probe's position and propagation direction as seen from Merritt Island gives us the residual doppler effect owing to earth rotation during the signal light time. At present the errors in these predictions cause the chief uncertainty in the experimental results.

the ground maser by sampling the output power at the antenna feed to minimize phase instability in the radiated signal. Tests involving the whole system were conducted during the month before the flight by using a dummy load at the antenna to ensure that the system was stable and that any diurnal phase variations that might occur would be well understood. Shortly before flight, the second reference maser was set up to monitor the primary reference for a direct comparison of frequency stability of the two masers.

No drifts of any significance to the experiment were observed during the time of the flight.

c) Frequency Corrections

The principal systematic frequency variation of the hydrogen masers is described by the following expression:

$$\frac{\Delta f}{f} = \frac{1}{f}\left[\frac{Q_c}{Q_\ell}\,(f_c - f_0) + 2750\,B^2\right] \quad . \tag{5}$$

The first term is the cavity-resonance mistuning, or "pulling," effect, and the second is the second-order magnetic-field dependence of the atomic hydrogen hyperfine transition $F = 1,\ M_F = 0 \rightarrow F = 0,\ M_F = 0$. Q_c is the cavity resonator Q and Q_ℓ is the Q of the atomic transition, which depends on the geometry of the hydrogen-maser storage bulb, the quality of the wall coating, and the collision rate of the atoms among themselves (spin-exchange processes). This last process is a function of beam input flux, which, in turn, can be represented in terms of maser output power level.

Two aspects of the cavity-resonance shift especially concern us: 1) the variation in Δf_c during the mission, and 2) the average magnitude of Δf_c as a result of the combination of shake, shock, and zero gravity that occur from earth-bound conditions through to the free-fall condition after powered flight ceases. The effect of cavity-resonance variations is obvious in equation (5). However, if there is also a large fixed offset $(f_c - f_0)$, we are further subject to output frequency variations due to variations in Q_ℓ resulting from changes in atomic hydrogen flux during the mission. These

The present best values for pressure, temperature, and rotation sensitivity on the output frequency of the maser are

$$\left.\frac{\Delta f}{f}\right|_{V,\Omega,W} = -2.9 \times 10^{-12}\ \Delta P \quad ,$$

$$\left.\frac{\Delta f}{f}\right|_{P,V,W} = -5.78 \times 10^{-17}\ \Delta\Omega^2 \quad ;$$

$$\left.\frac{\Delta f}{f}\right|_{P,\Omega,W} = -3.6 \times 10^{-14}\ \Delta V \quad ,$$

where ΔP is in psi and Ω is in rev/min.

This last calibration, which is for temperature, is given in terms of the aft-oven heater voltage, which was servo-controlled to remain constant at the most temperature-sensitive region of the maser.

The effect of the power-level variation is

$$\left.\frac{\Delta f}{f}\right|_{V,\Omega,P} = 1.22 \times 10^{-7}\ \Delta f_c\ \Delta W \quad ,$$

where ΔW is in ergs/sec and f_c is in Hz. In these calculations, values of $Q_c = 3.4 \times 10^4$ and $Q_\ell = 1.11 \times 10^9$ were determined for the probe flight for conditions of operation.

During prelaunch testing at MSFC, we established the offset frequency between the probe maser and the ground masers under the conditions at which the probe would be operated. This fixed offset was chiefly due to wall-shift variations in the bulb

Calibrations were made of transponder output phase versus input signal level over the range expected during the flight. Similar phase calibrations were made on the ground-based receivers that were to handle the transponder and translator downlink signals.

The antenna systems were also calibrated. As mentioned earlier, the probe antenna was an on-axis dipole in order to minimize the effect of payload rotation. This antenna was located in a 10° conical ground plane aft of the payload as part of the attachment to the fourth rocket stage. The remaining payload was enclosed in a carefully designed symmetrical shield, which served as a rotationally symmetrical extension of the antenna ground plane and as a thermal-radiation shield.

The phase variations of the probe antenna with aspect angle and roll angle about the spin axis were measured for each of the three frequencies. The residual phase error that would result from processing via the doppler-canceling system will be calculated as a function of aspect angle. This error is due to the fact that the antenna aspect phase patterns were not exactly identical for each frequency. (The roll patterns were very uniform and present no problem.)

e) Ground-Station Equipment

The ground station at Merrit Island had two VLG-10A masers built at SAO specially for the experiment; a third maser was located at Wallops Island. The environment for all the masers was carefully controlled, and the relative frequencies of the masers at Merrit Island were constantly monitored. At this time, it appears that the ground station masers contributed a systematic error of less than 1×10^{-14} during the flight.

TABLE 1

Time	$\frac{\dot{r}}{c}$	$\frac{\Delta f}{f_0}$	$\frac{\Delta c}{c}$
1148	2.06×10^{-5}	-2×10^{-13}	1.9×10^{-8}
1240	-Apogee-		
1322	-1.23×10^{-5}	2×10^{-14}	-3.2×10^{-9}
1334	-1.07×10^{-5}	3×10^{-13}	-5.6×10^{-8}

By taking the slope of the phase residuals and thus obtaining the frequency residual, we can estimate the significance of the experiment as a test of the equivalence principle. Figure 20 shows, on the same time axis, both the frequency residuals and the $\Delta\Phi/c^2$ encountered by the probe maser.

Starting at 12:20 GMT, when the probe system appears to have stabilized from the trauma of launch, and ending with the data at 13:22 GMT, when the power supply to the ground-station uplink transmitter failed, we estimate that the relationship

$$\frac{\frac{\Delta f}{f_0}}{\frac{\Delta \Phi}{c^2}} = 1 \pm 2 \times 10^{-4}$$

and that over this part of the trajectory the tracking accuracy is consistent with this value.

It is clear that a great deal of data analysis remains and that this report is preliminary in nature. We can now assert that a space-qualified hydrogen maser has indeed been operationally demonstrated and that a doppler-canceling system that also cancels the gross effects of ionospheric refractive-index variations has been validated. In addition there is to be noted that, if the validity of the principle of equivalence is assumed to be correct, we can place an upper bound on the ratio of the one-way to the two-way velocity of light.

If we ascribe the total frequency residual to an assymmetry in the velocity of light we would expect the signature of the residual frequency discrepancy to replicate the first order doppler frequency in the manner described by equation (2). At the present stage of the data analysis the signature of the frequency residual shown in figure 19, does not resemble the doppler and the best we can do to answer the velocity of light question is to set an upper bound on the magnitude of Δc as is pertains to this experiment.

Assuming the validity of the equivalence principle and ascribing all the residual frequency to the assymmetry of the velocity of light we can set upper bounds to the value of $\frac{\Delta c}{c}$ as follows in table I.

Acknowledgment

This work was supported in part by Contract NAS8-27969 from the National Aeronautics and Space Administration/Marshall Space Flight Center.

References and Bibliography

Blamont, J. E., and Rodier, F., 1961, Phys. Rev. Lett., vol. 7, p. 437.

Brault, J. W., 1962, Ph.D. Thesis, Princeton Univ.

Einstein, A., 1911, Ann. Phys. (Leipzig), vol. 35, p. 898.

Pound, R. V., and Rebka, G. A., Jr., 1960, Phys. Rev. Lett., vol. 4, p. 337.

Pound, R. V., and Snider, J. L., 1965, Phys. Rev., vol. 140B, p. 788.

Rodier, F., 1965, Ann. Astrophys., vol. 28, p. 463.

Snider, J. L., 1970, Solar Phys., vol. 12, p. 352.

Snider, J. L., 1972, Phys. Rev. Lett., vol. 28, p. 853.

Vessot, R. F. C., 1974, in Experimental Gravitation, ed. by B. Bertotti, Academic Press, New York, p. 111.

Similarly we can approximate equation A-1 and get

$$f' = f_0 \left[1 + \frac{\phi_2 - \phi_3}{c^2} - \text{etc} \right] \left[1 - (\vec{\beta}_3 - \vec{\beta}_2) \cdot \vec{\epsilon}_{23} \right]$$

$$\frac{f' - f_0}{f_0} \doteq \left[\frac{\phi_2 - \phi_3}{c^2} - \text{etc} \right] + \frac{\dot{r}_{23}}{c_{23}}$$

The output from the last mixer in the schematic diagram shown as Figure 5 gives

$$\frac{\Delta f_c}{f_0} = \frac{1}{f_0} \left[f' - f_0 - \frac{f'' - f_0}{2} \right]$$

$$\doteq \frac{\Delta f}{f_0} + \frac{\dot{r}_{23}}{c_{23}} + \frac{\dot{r}_{12}}{2c_{12}} - \frac{\dot{r}_{23}}{2c_{23}}$$

$$\doteq \frac{\Delta f}{f_0} + \frac{\dot{r}}{2} \left[\frac{1}{c_{12}} - \frac{1}{c_{23}} \right]$$

Where $\dot{r}_{12} = -\dot{r}_{23}$ and is designated by $\dot{r}$, the range rate. If we write $\Delta c = c_{23} - c_{12}$ we have

$$\frac{\delta f_c}{f_0} \doteq \frac{\Delta f}{f_0} + \frac{\dot{r}}{2c} \frac{\Delta c}{c}$$

At the present stage of our data reduction if we ascribe all the experimentally observed departure of the frequency residual to a possible anisotropy in the velocity of light we can set an upper bound for this quantity as it pertains to the conditions that existed during the experiment.

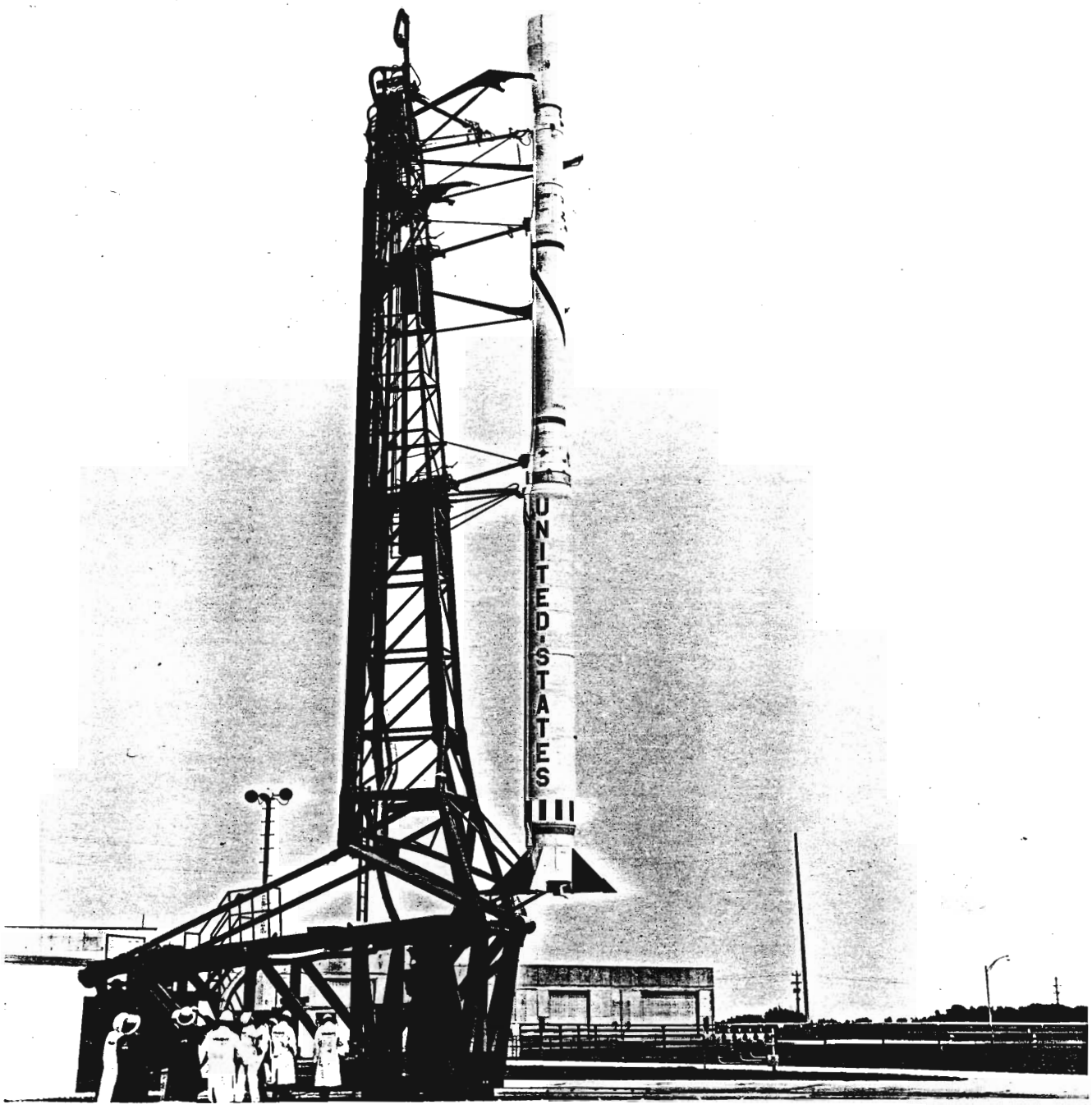

Figure 1.

NASA Wallops Flight Center
W1-76-478

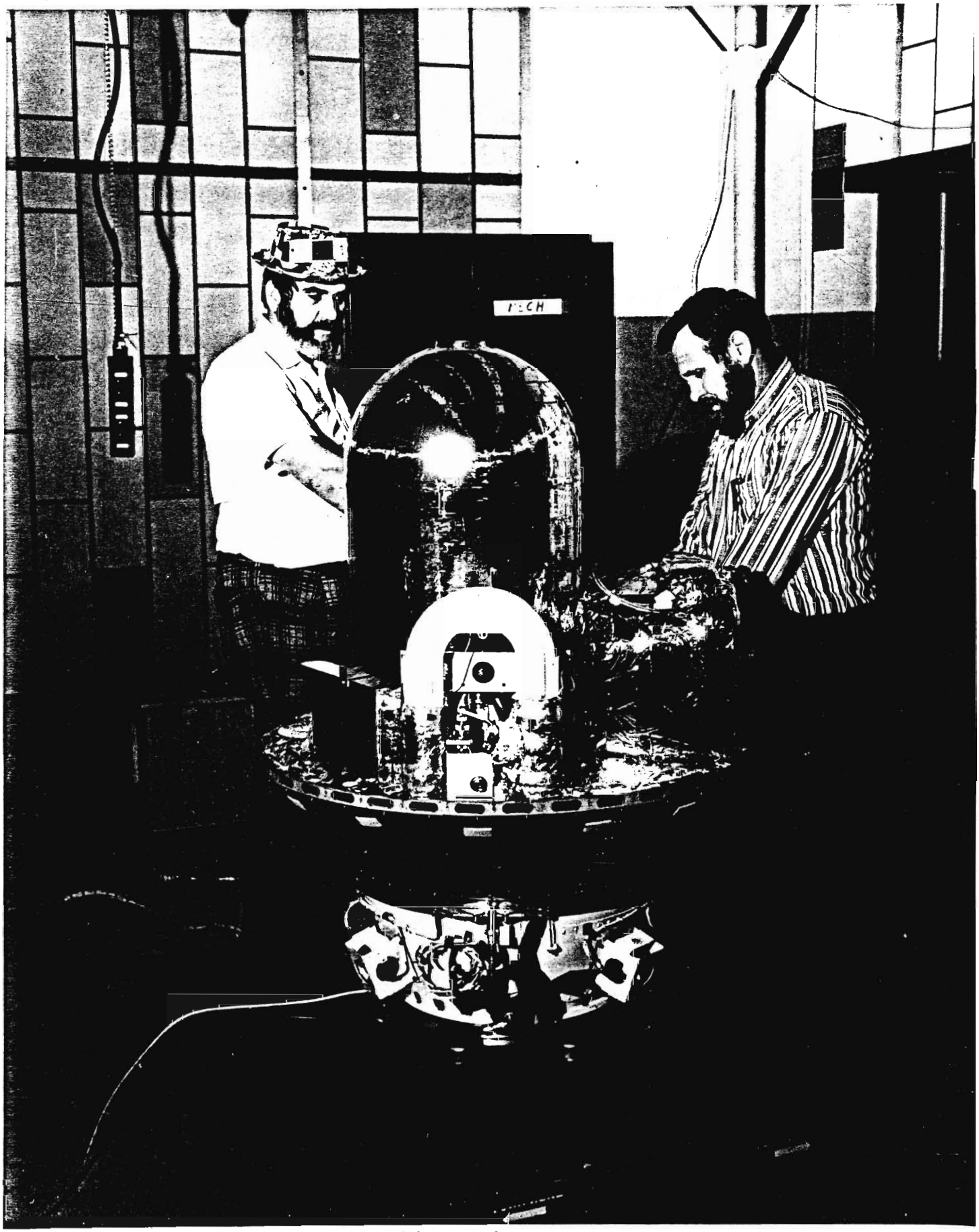

Figure 2.

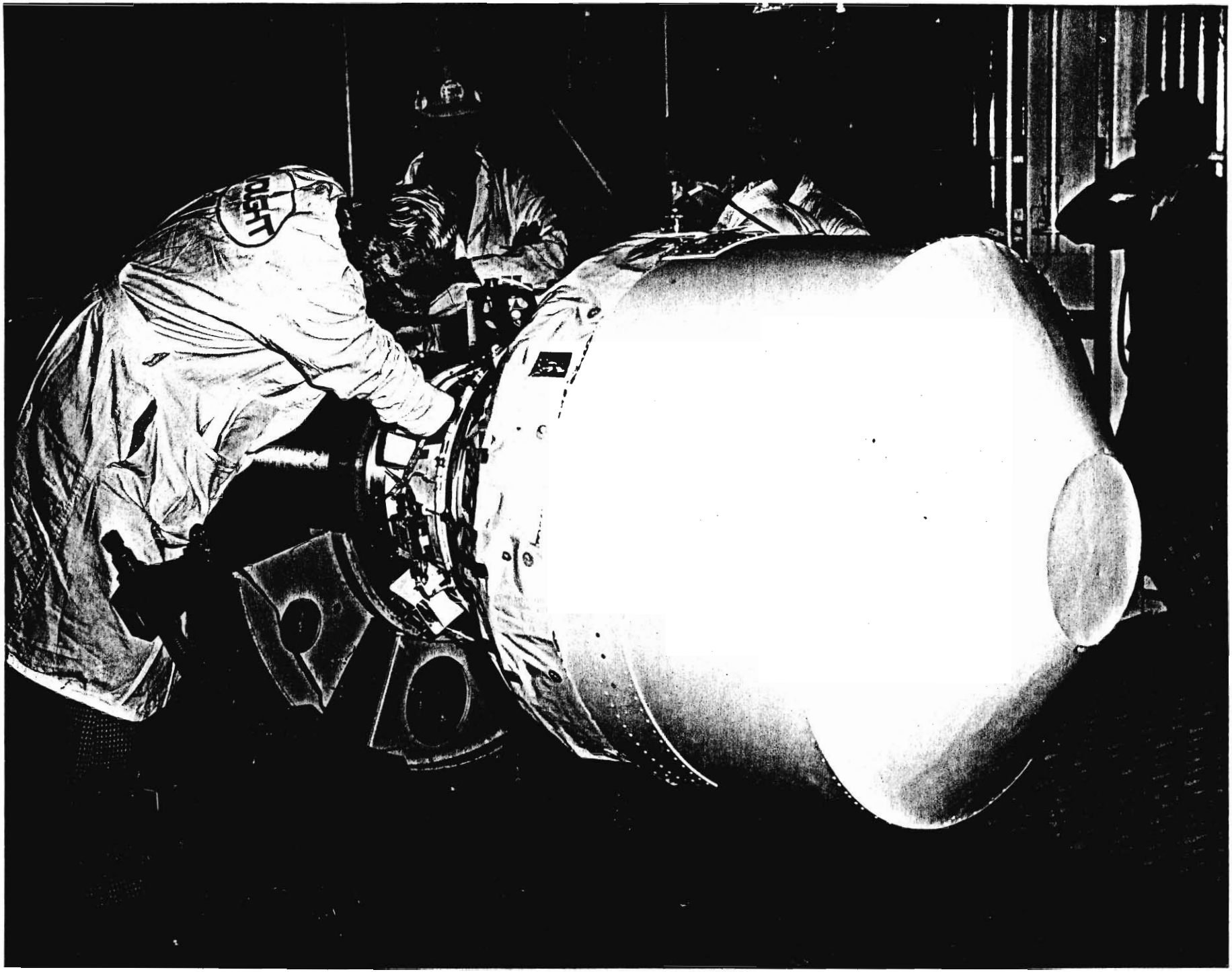

Figure 3.

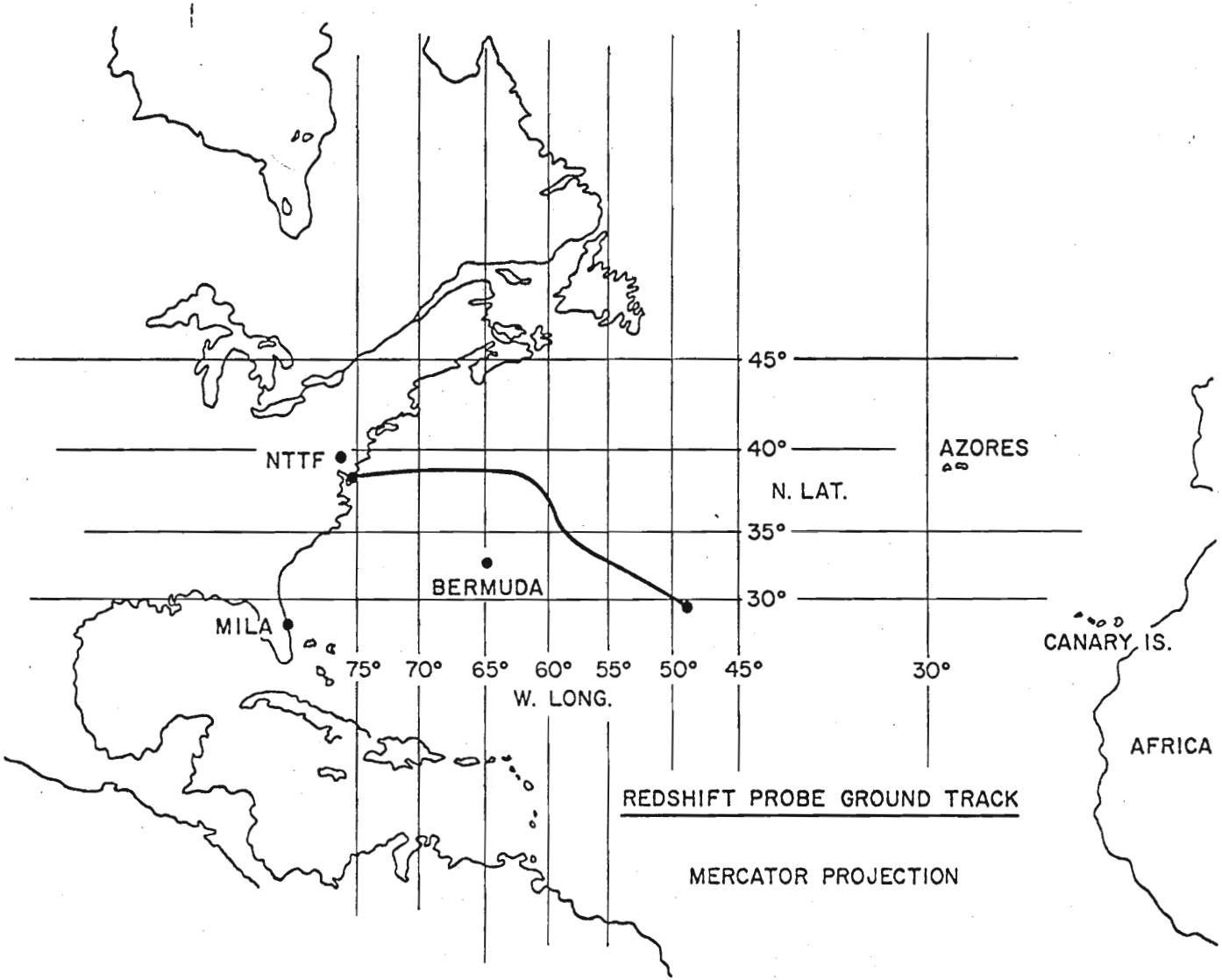
45°
40°
35°
30°
N. LAT.
NTTF
AZORES
BERMUDA
MILA
CANARY IS.
AFRICA
75° 70° 65° 60° 55° 50° 45° 30°
W. LONG.
REDSHIFT PROBE GROUND TRACK
MERCATOR PROJECTION

Figure 4

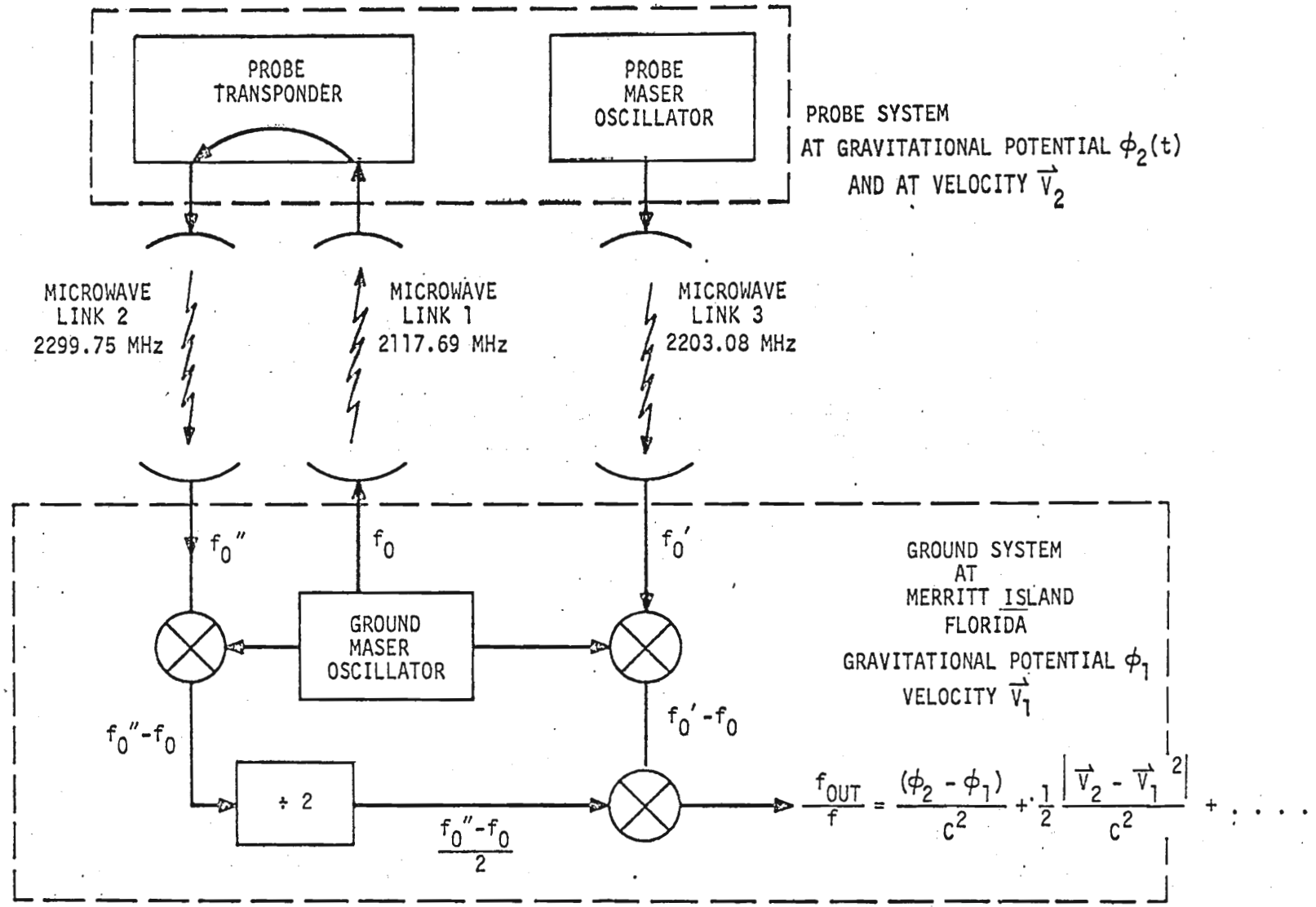

REDSHIFT EXPERIMENT DOPPLER CANCELLING SYSTEM

Figure 5

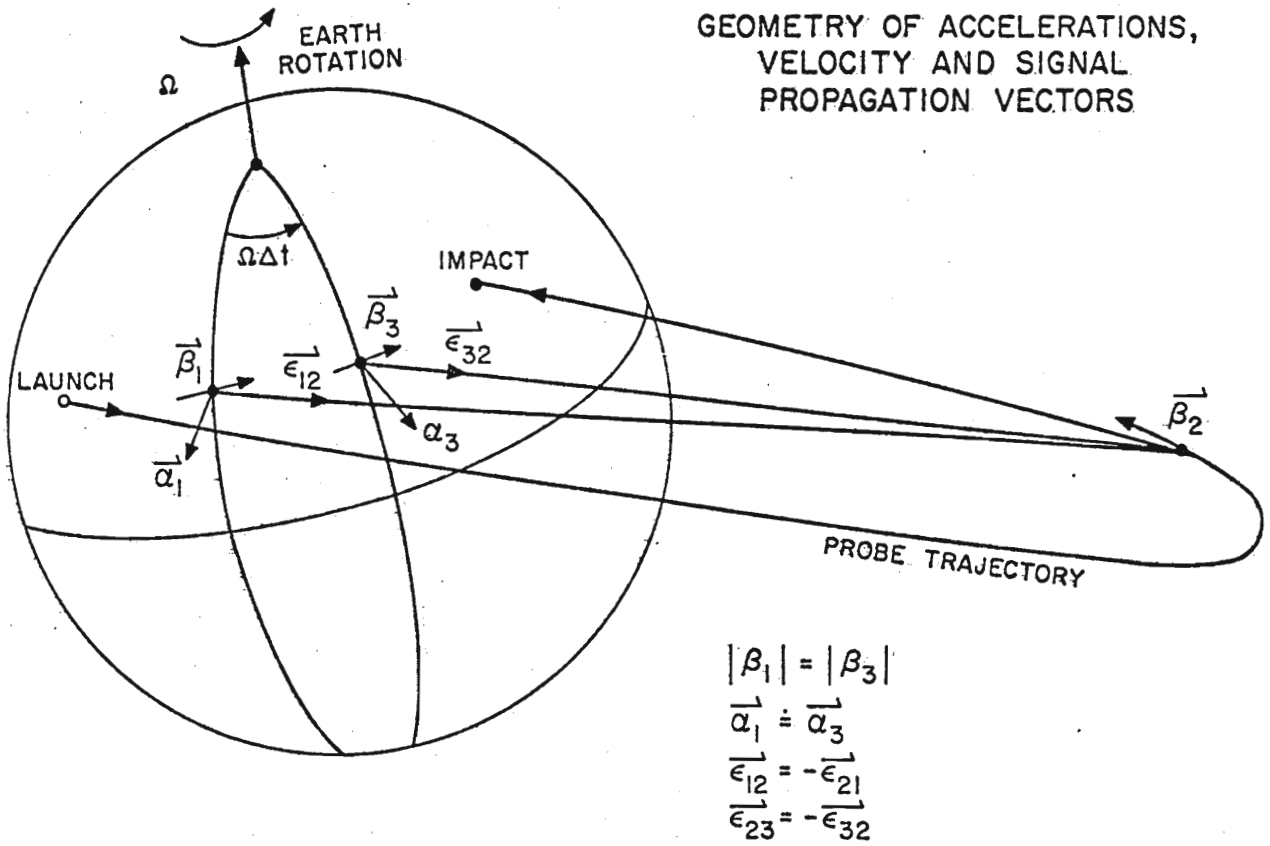
GEOMETRY OF ACCELERATIONS,
VELOCITY AND SIGNAL
PROPAGATION VECTORS
EARTH
ROTATION
Ω
ΩΔt
IMPACT
LAUNCH
$\vec{\beta}_1$
$\vec{\epsilon}_{12}$
$\vec{\beta}_3$
$\vec{\epsilon}_{32}$
$\vec{\beta}_2$
α_3
$\vec{\alpha}_1$
PROBE TRAJECTORY
$|\beta_1| = |\beta_3|$
$\vec{\alpha}_1 \doteq \vec{\alpha}_3$
$\vec{\epsilon}_{12} = -\vec{\epsilon}_{21}$
$\vec{\epsilon}_{23} = -\vec{\epsilon}_{32}$

Figure 6

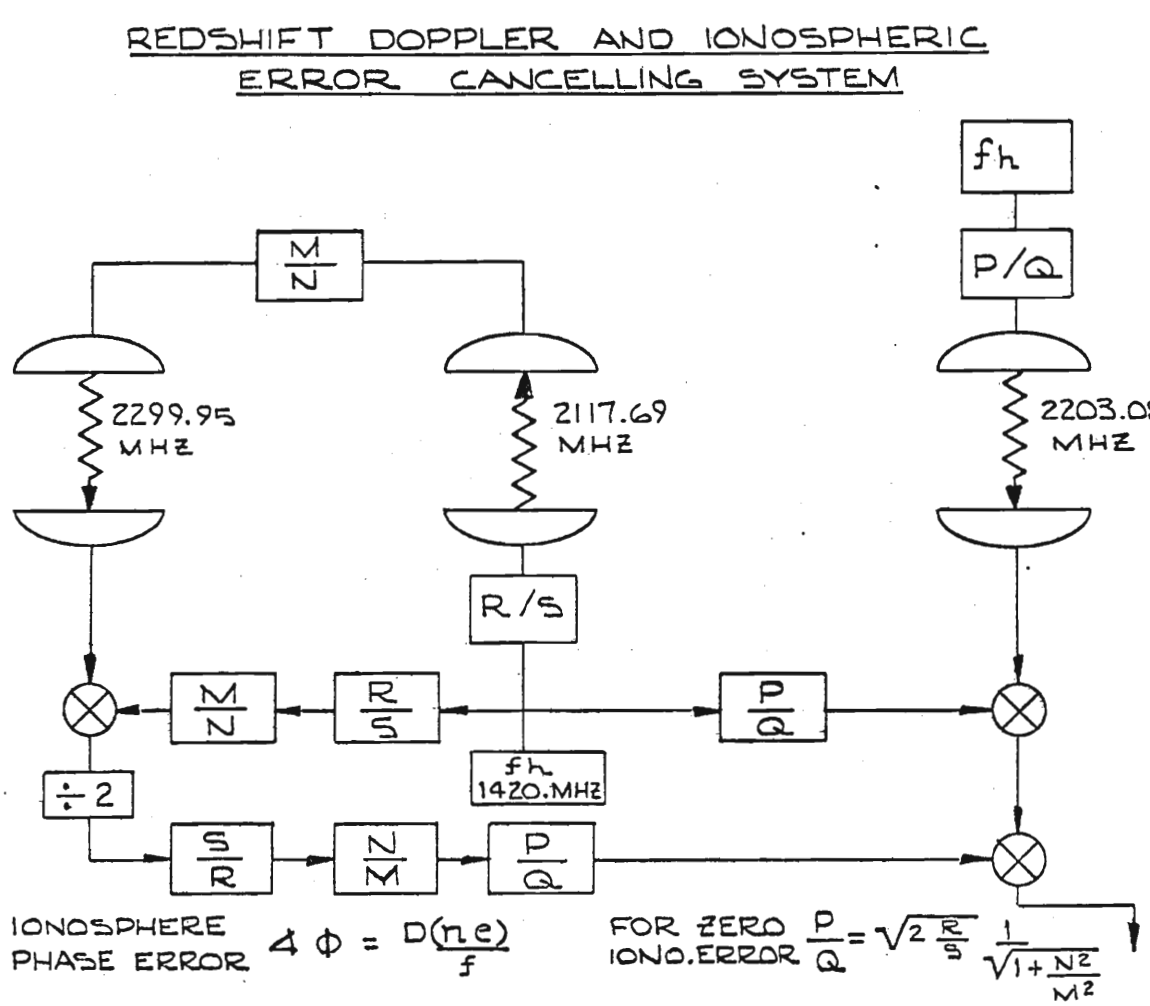
REDSHIFT DOPPLER AND IONOSPHERIC
ERROR CANCELLING SYSTEM
fh
P/Q
M/N
2299.95
MHz
2117.69
MHz
2203.08
MHz
R/S
M/N
R/S
P/Q
fh
1420.MHz
÷2
S/R
N/M
P/Q
IONOSPHERE
PHASE ERROR
$\Delta\Phi = \frac{D(n_e)}{f}$
FOR ZERO
IONO.ERROR
$\frac{P}{Q} = \sqrt{2}\,\frac{R}{S}\,\frac{1}{\sqrt{1+\frac{N^2}{M^2}}}$

Figure 7

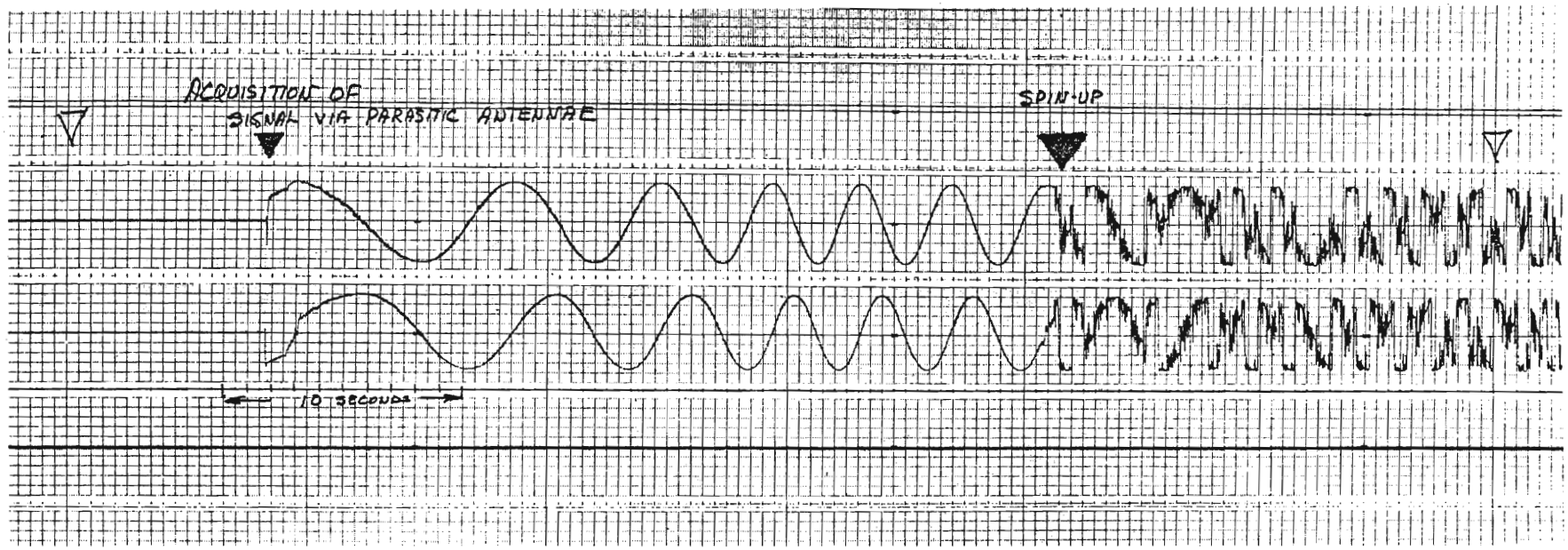
ACQUISITION OF
SIGNAL VIA PARASITIC ANTENNAE
SPIN-UP
10 SECONDS

Fig. 8

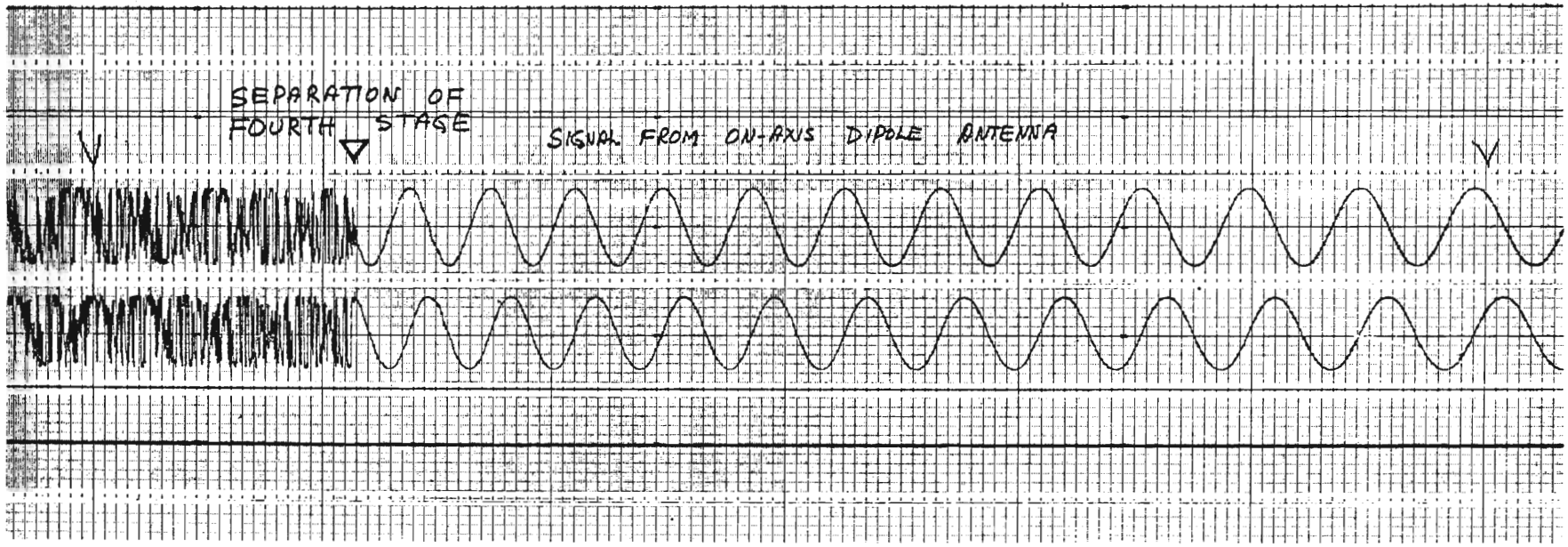
SEPARATION OF
FOURTH STAGE
SIGNAL FROM ON-AXIS DIPOLE ANTENNA

Fig. 9

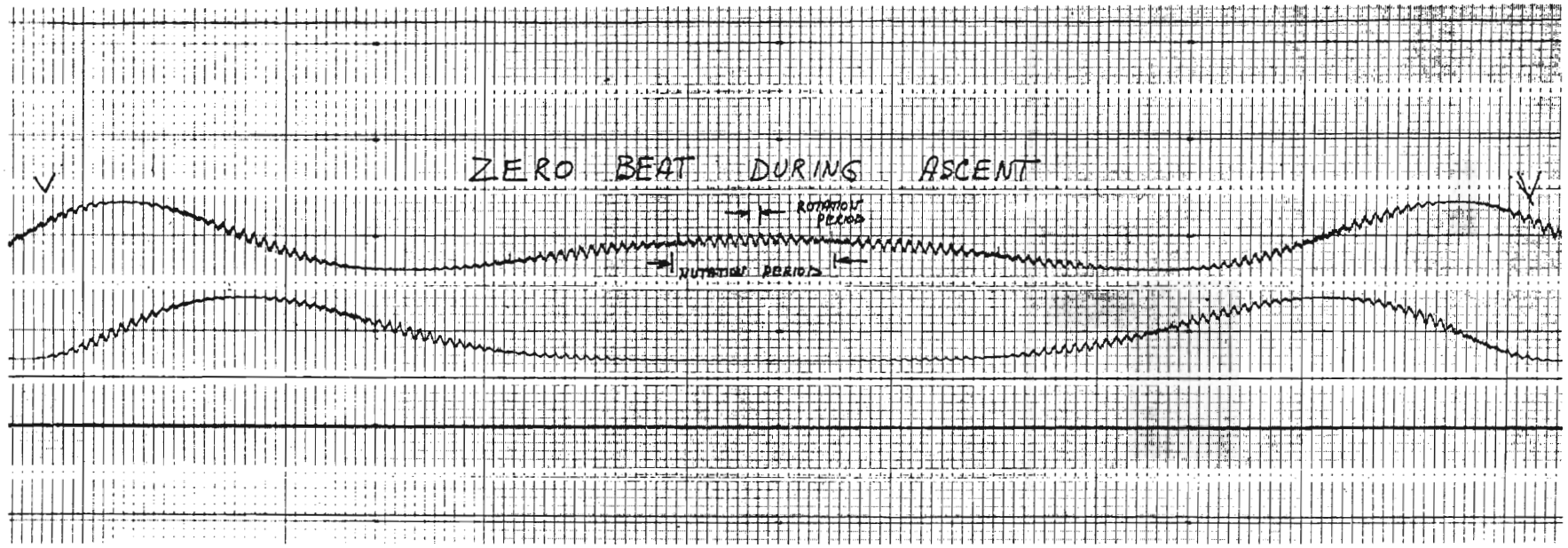

Fig. 10

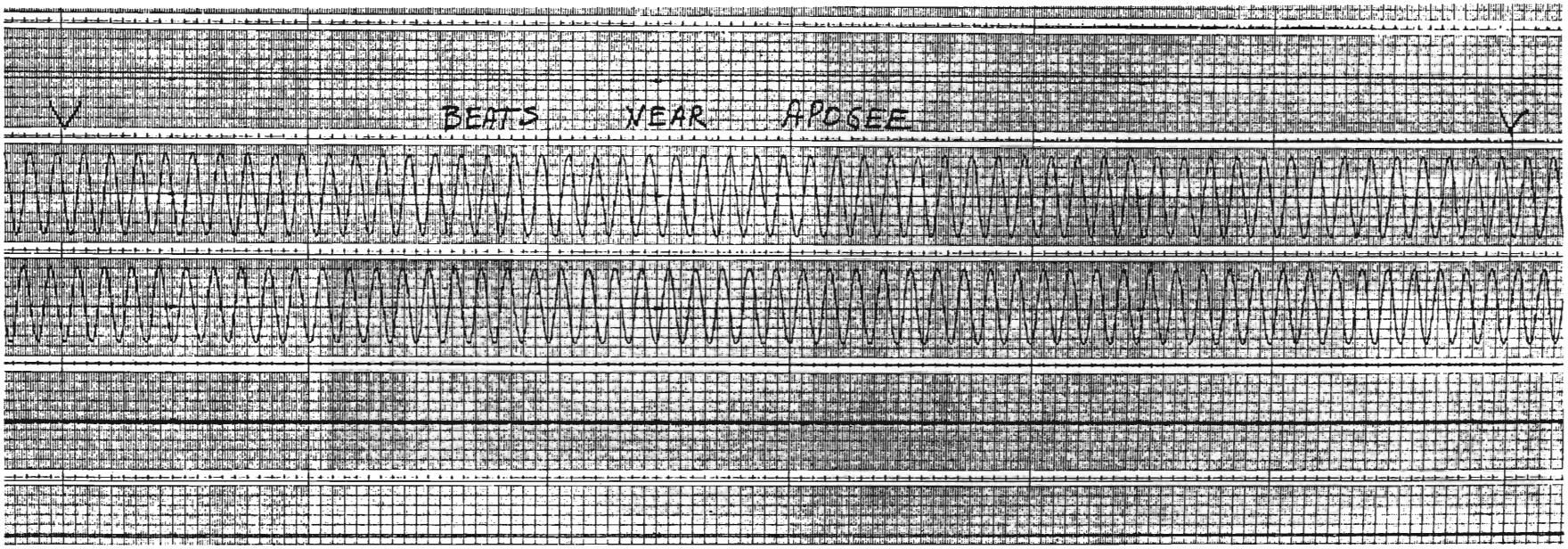

Fig. 1

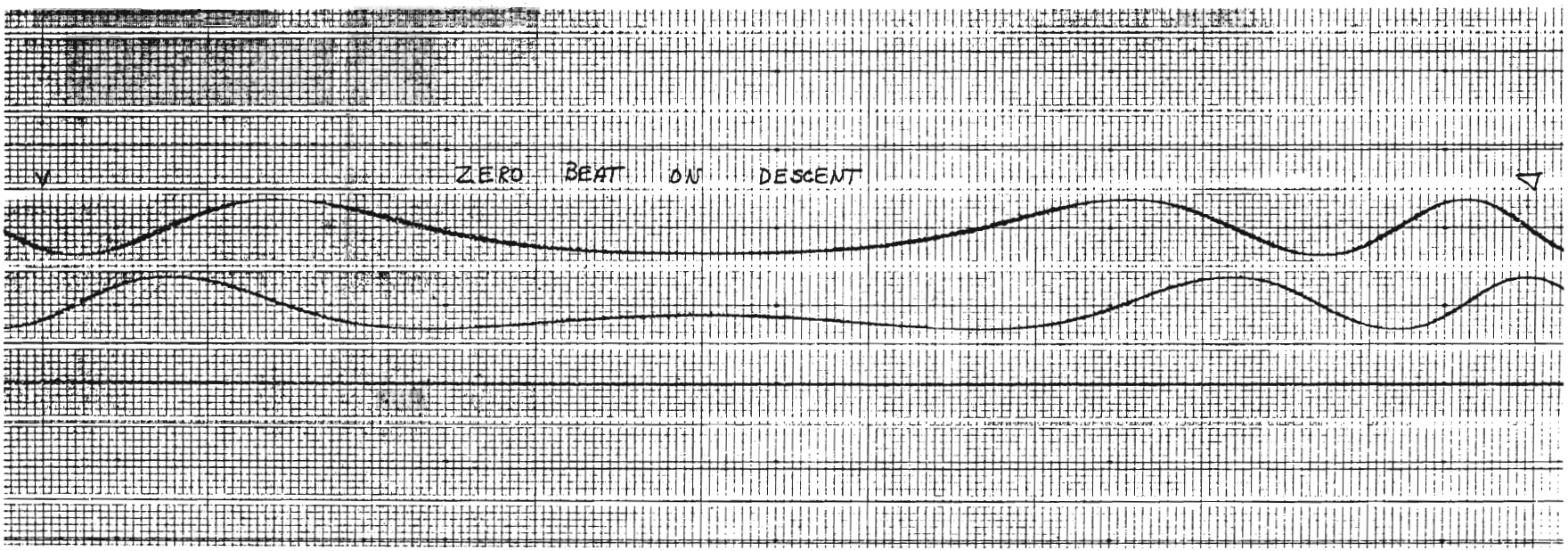

Fig.12

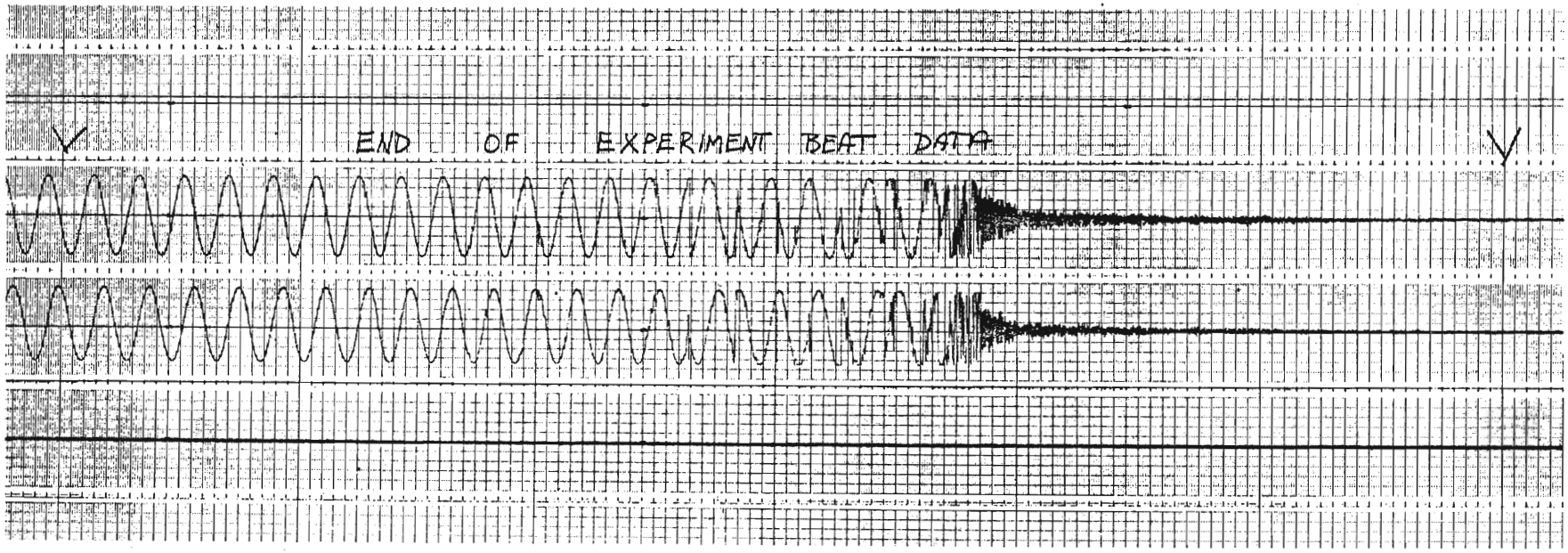

Fig. 13

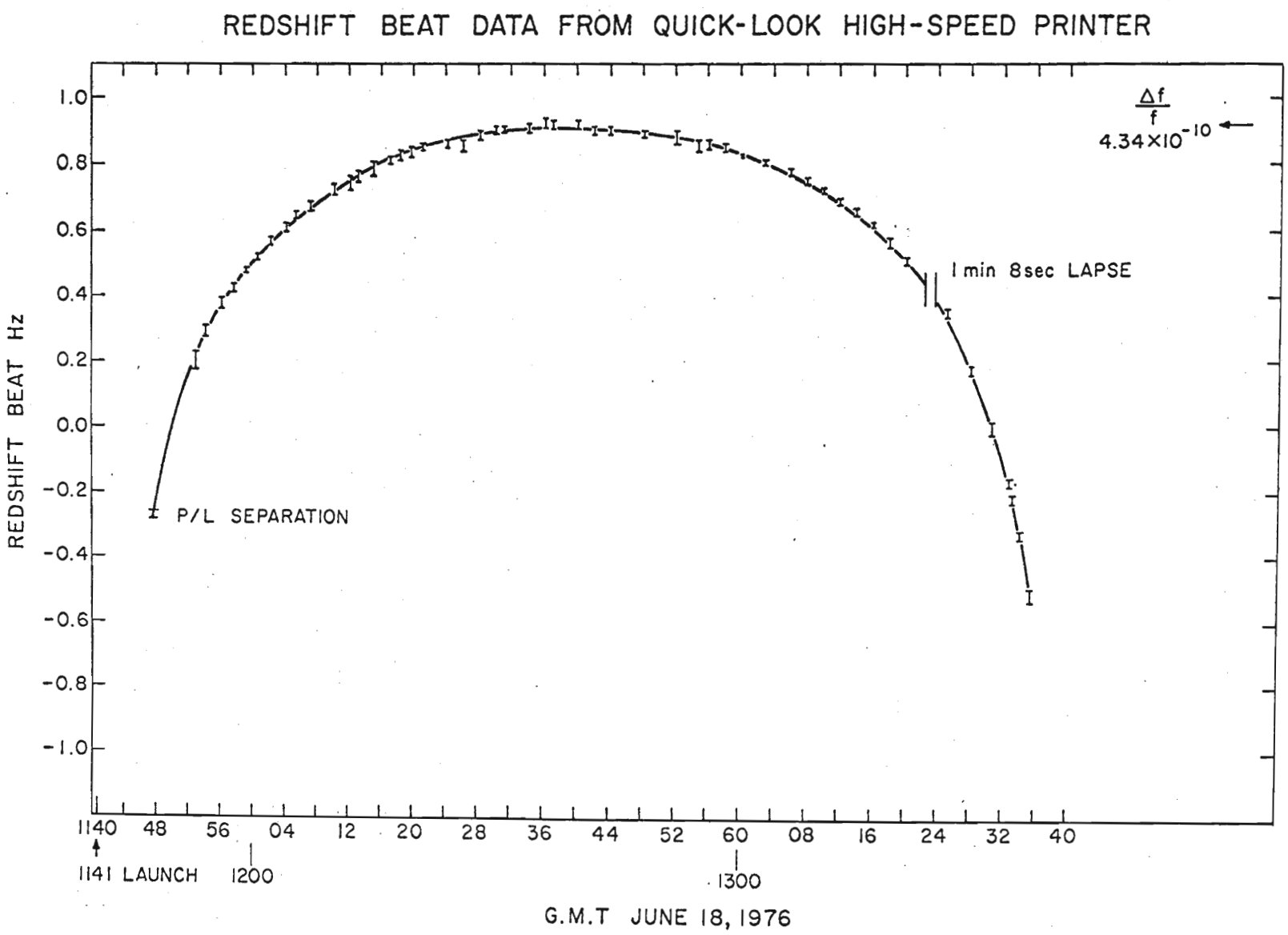
REDSHIFT BEAT DATA FROM QUICK-LOOK HIGH-SPEED PRINTER
REDSHIFT BEAT Hz
1.0
0.8
0.6
0.4
0.2
0.0
-0.2
-0.4
-0.6
-0.8
-1.0
Δf/f
4.34×10⁻¹⁰
1 min 8sec LAPSE
P/L SEPARATION
1140
48
56
04
12
20
28
36
44
52
60
08
16
24
32
40
1141 LAUNCH
1200
1300
G.M.T JUNE 18, 1976

Figure 14

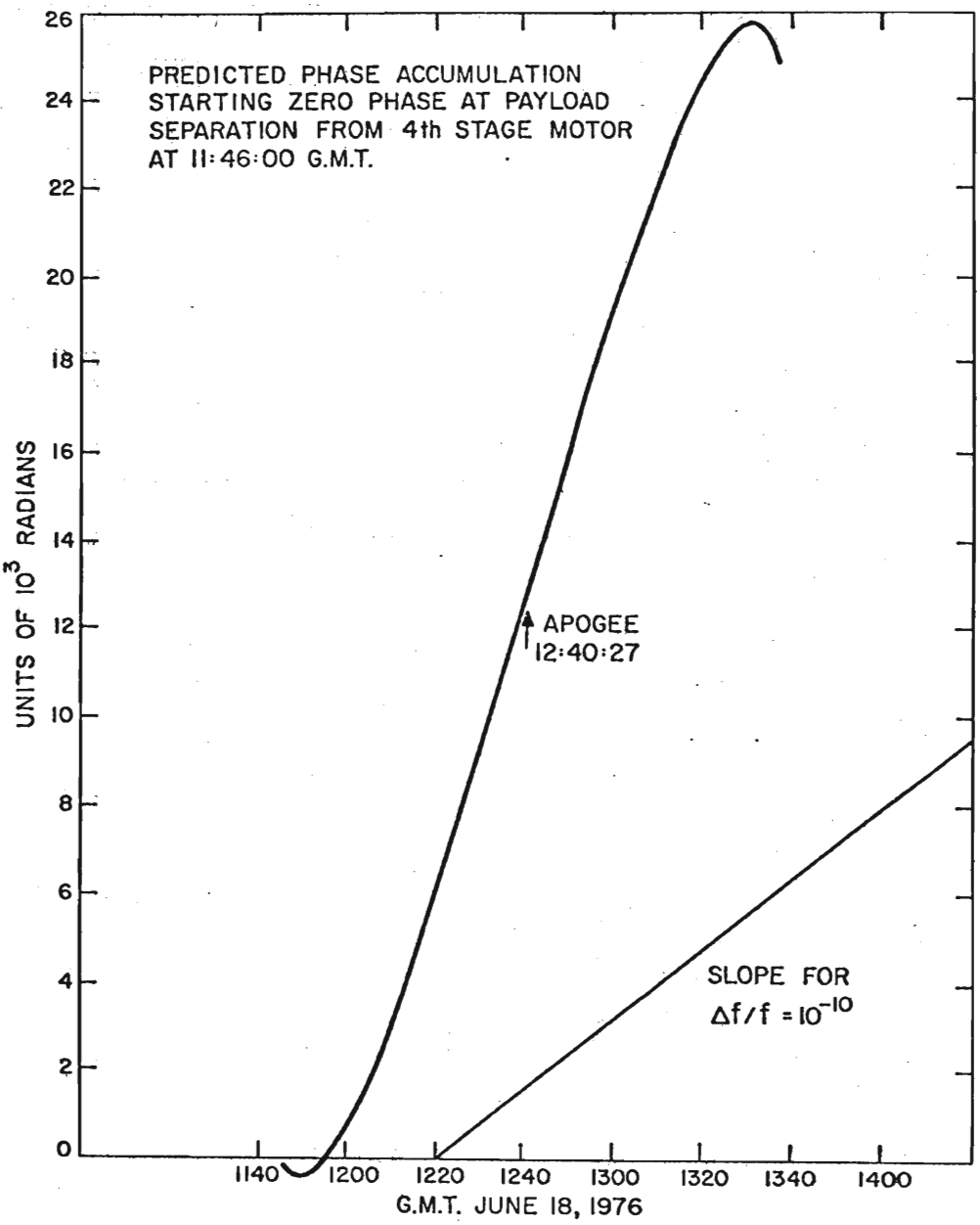
PREDICTED PHASE ACCUMULATION
STARTING ZERO PHASE AT PAYLOAD
SEPARATION FROM 4th STAGE MOTOR
AT 11:46:00 G.M.T.
APOGEE
12:40:27
SLOPE FOR
Δf/f = 10^-10
UNITS OF 10^3 RADIANS
0
2
4
6
8
10
12
14
16
18
20
22
24
26
1140
1200
1220
1240
1300
1320
1340
1400
G.M.T. JUNE 18, 1976

Figure 15

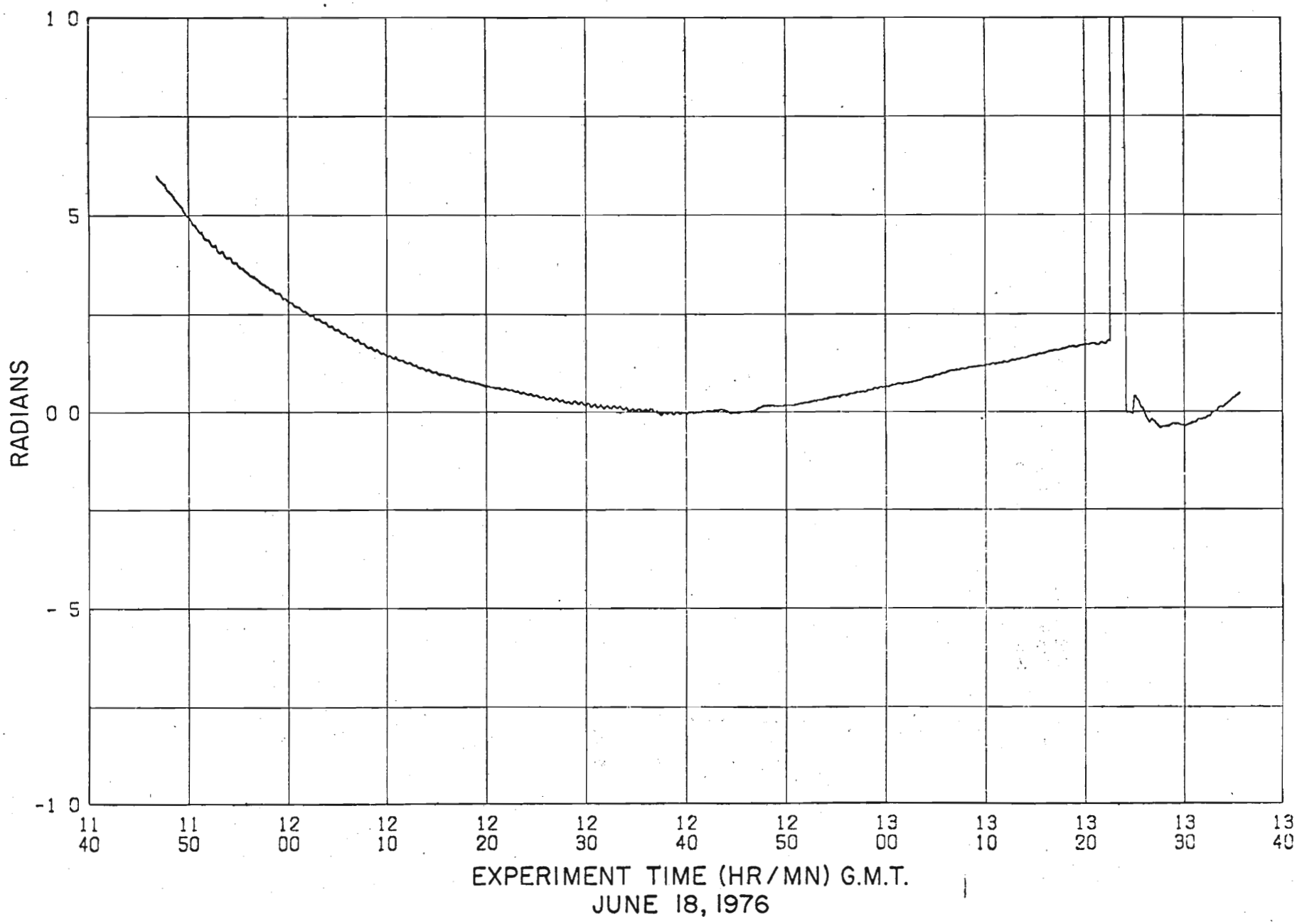
REDSHIFT PHASE RESIDUALS
5 × 10^-13 SLOPE REMOVED
1 0
5
0 0
- 5
-1 0
RADIANS
11 40
11 50
12 00
12 10
12 20
12 30
12 40
12 50
13 00
13 10
13 20
13 30
13 40
EXPERIMENT TIME (HR/MN) G.M.T.
JUNE 18, 1976

Figure 16

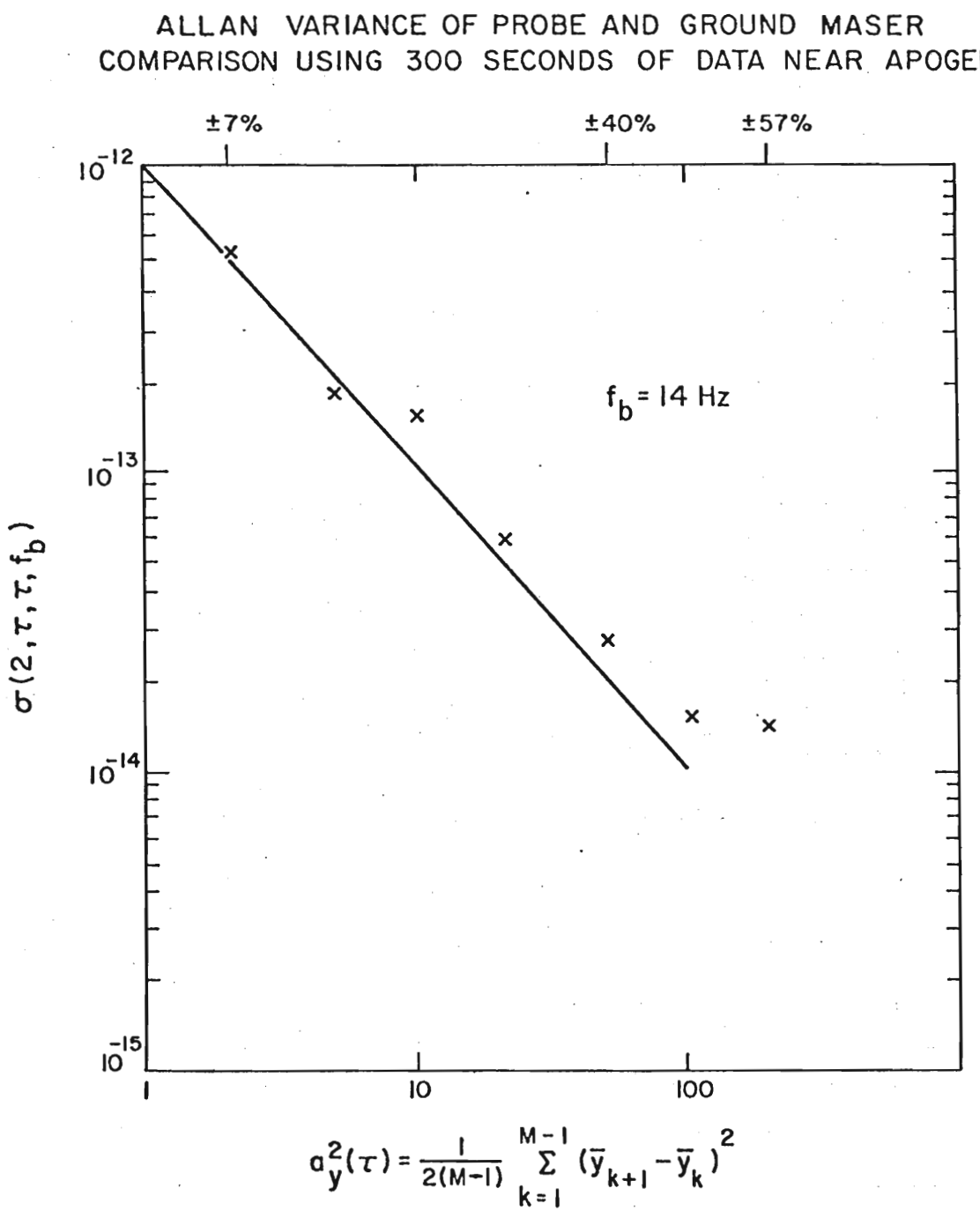
ALLAN VARIANCE OF PROBE AND GROUND MASER
COMPARISON USING 300 SECONDS OF DATA NEAR APOGEE
±7%
±40%
±57%
10^{-12}
10^{-13}
10^{-14}
10^{-15}
f_b = 14 Hz
$\sigma(2,\tau,\tau,f_b)$
1
10
100
$a_y^2(\tau) = \frac{1}{2(M-1)} \sum_{k=1}^{M-1} (\bar{y}_{k+1} - \bar{y}_k)^2$

Figure 17

PHASE CORRECTIONS FROM MAG. FIELD & TELEMETRY DATA

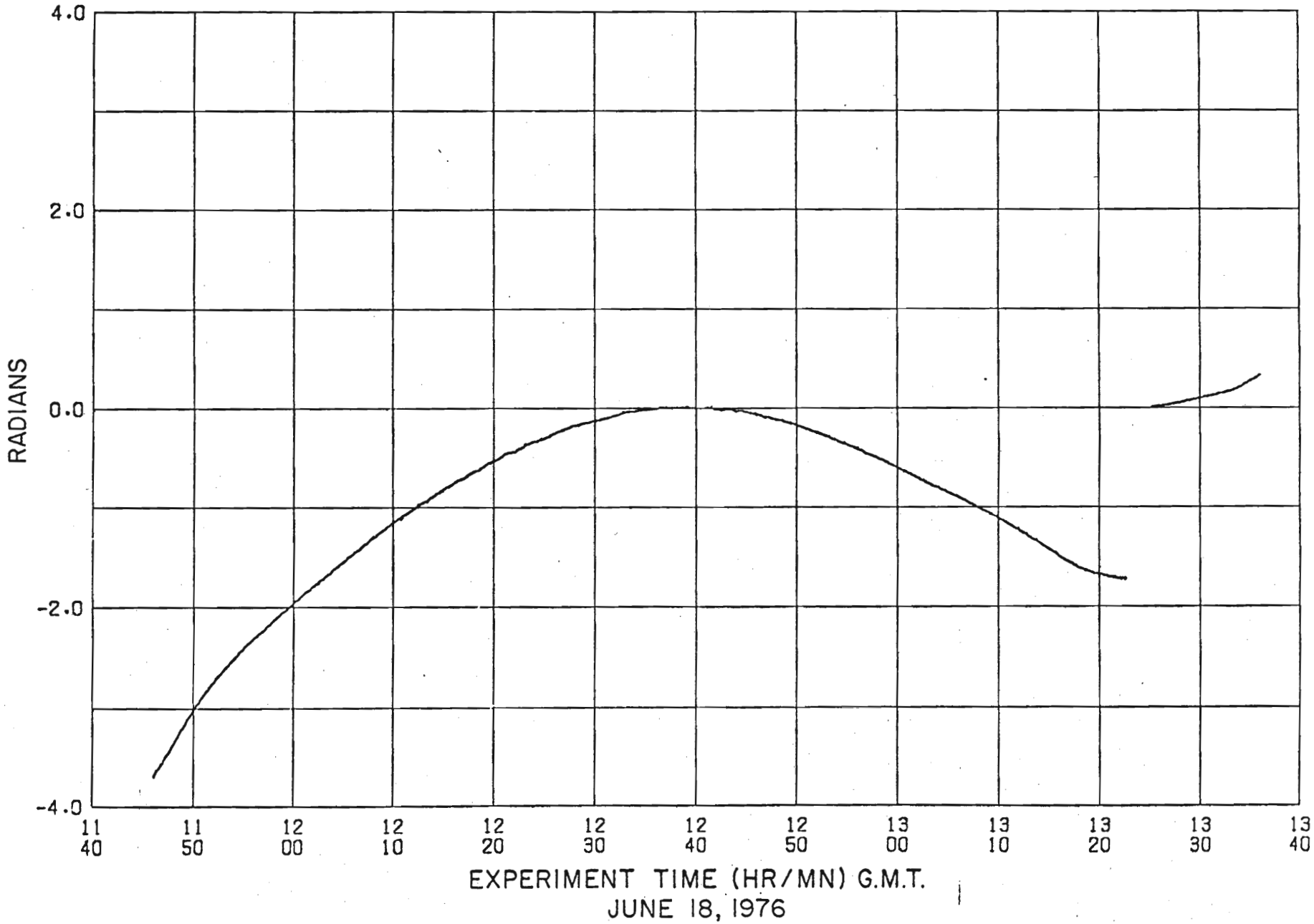

Figure 18

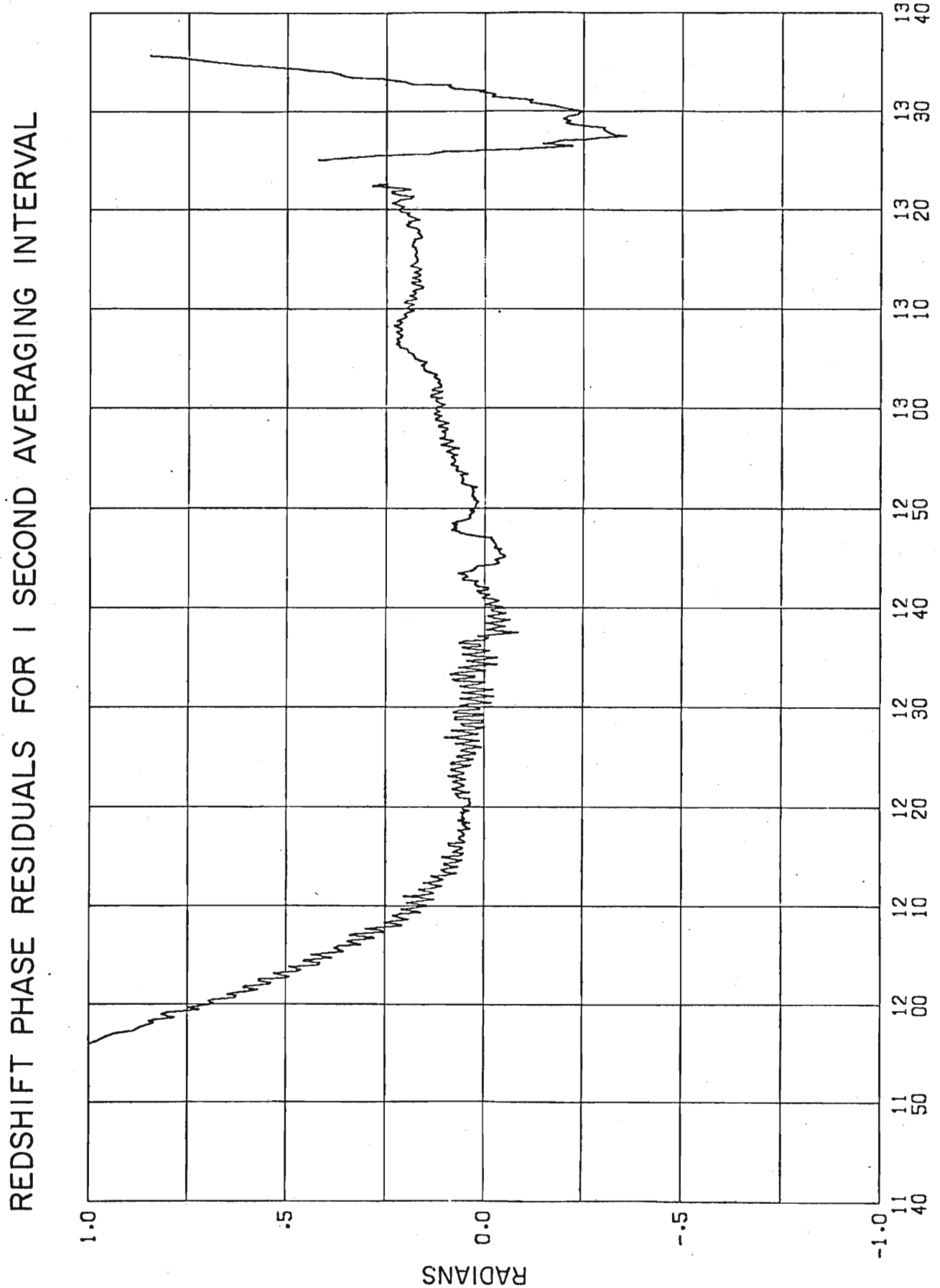
REDSHIFT PHASE RESIDUALS FOR 1 SECOND AVERAGING INTERVAL
RADIANS
1.0
.5
0.0
-.5
-1.0
11 40
11 50
12 00
12 10
12 20
12 30
12 40
12 50
13 00
13 10
13 20
13 30
13 40
EXPERIMENT TIME (HR/MN) G.M.T.
JUNE 18, 1976

Figure 19

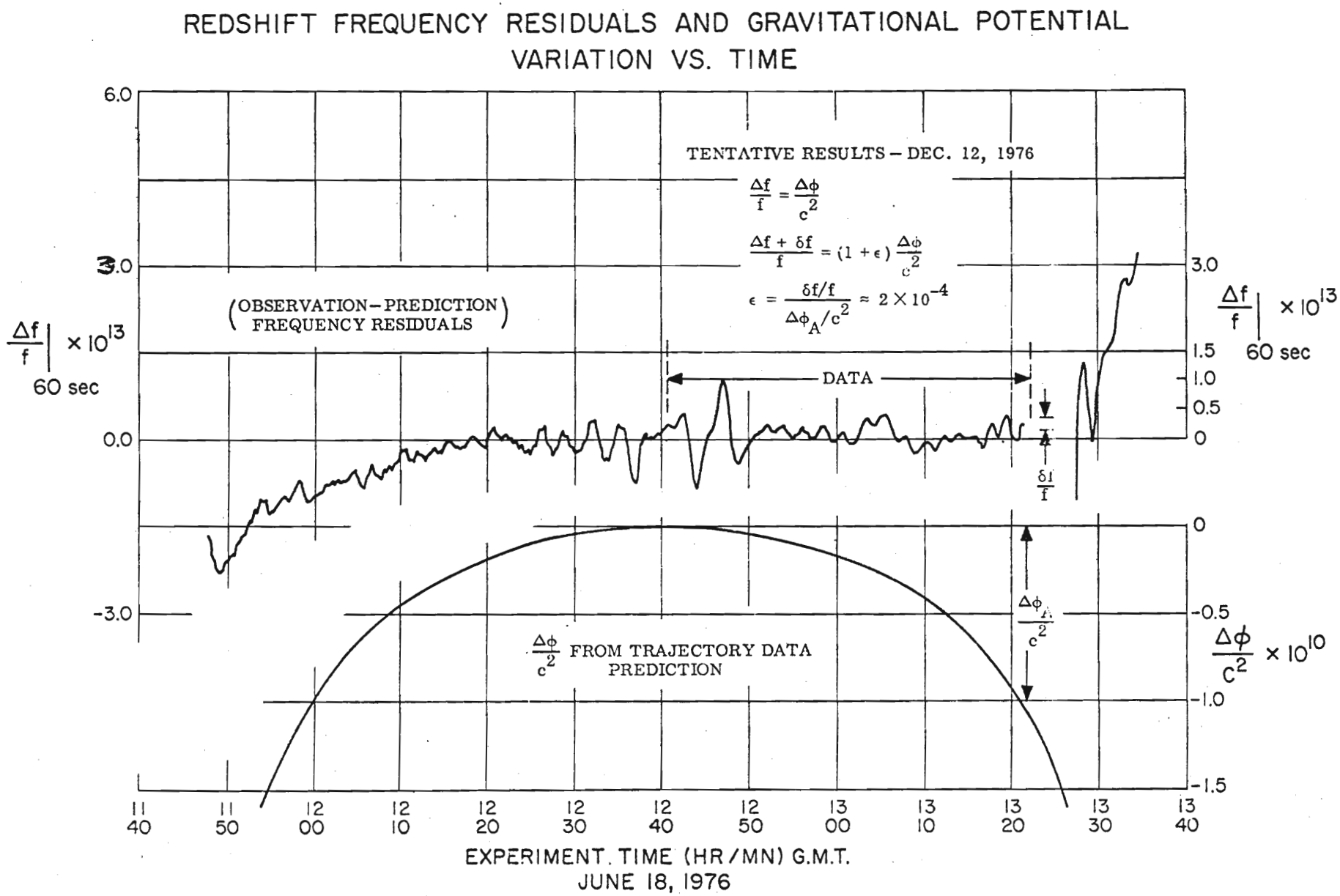
REDSHIFT FREQUENCY RESIDUALS AND GRAVITATIONAL POTENTIAL VARIATION VS. TIME
TENTATIVE RESULTS – DEC. 12, 1976
$\frac{\Delta f}{f} = \frac{\Delta \phi}{c^2}$
$\frac{\Delta f + \delta f}{f} = (1 + \epsilon)\frac{\Delta \phi}{c^2}$
$\epsilon = \frac{\delta f/f}{\Delta \phi_A / c^2} \approx 2 \times 10^{-4}$
(OBSERVATION – PREDICTION FREQUENCY RESIDUALS)
DATA
$\frac{\delta f}{f}$
$\frac{\Delta f}{f} \times 10^{13}$ 60 sec
$\frac{\Delta \phi_A}{c^2}$
$\frac{\Delta \phi}{c^2}$ FROM TRAJECTORY DATA PREDICTION
$\frac{\Delta \phi}{c^2} \times 10^{10}$
6.0
3.0
0.0
-3.0
1.5
1.0
0.5
0
-0.5
-1.0
-1.5
11 40
11 50
12 00
12 10
12 20
12 30
12 40
12 50
13 00
13 10
13 20
13 30
13 40
EXPERIMENT. TIME (HR/MN) G.M.T.
JUNE 18, 1976

Figure 20

SUMMARY

An experimental verification of Einstein's equivalence principle has been made using an atomic hydrogen maser in a space probe attaining an altitutde of 10,000 km about the earth's surface. At the present stage of the data reduction confirmation is at the 2×10^{-4} level of accuracy. The experiment and the resulting data are described including a comment on the limits to the anisotropy of the velocity of light. The authors believe that this is the first direct, high accuracy test of the question of symmetry in the propagation of light in addition to being a beginning in the use of high accuracy clocks in space to measure relativistic phenomena.

BIOGRAPHICAL SKETCH

Martin W. Levine

Martin W. Levine was born in Jersey City, N.Y., on July 4, 1932. He received the B.S.E.E. and M.S.E.E. degrees from the Massachusetts Institute of Technology, Cambridge, in 1954 and the Ph.D. degree in electrical engineering from Purdue University, Lafayette, Ind., in 1965.

From 1966 to 1969 he was employed by Hewlett-Packard, Beverly, Mass., where he worked on the development of atomic frequency standards. Since 1969, he has continued development of the atomic hydrogen maser at the Smithsonian Astrophysical Observatory, Cambridge, Mass.

Robert F. C. Vessot

Robert F. C. Vessot was born in Montreal, Que., Canada on April 16, 1930. He received the B.S., M.S., and Ph.D. degrees in physics, from McGill University, Montreal, Que., in 1951, 1954, and 1957, respectively.

From 1956 to 1960 he was a Staff Member of the Department of Sponsored Research, Massachusetts Institute of Technology, Cambridge, where he worked on cesium beam frequency standards as well as on a cold helium gas moderated cesium maser. Shortly after joining Varian Associates, Beverly, Mass., in 1960, he initiated a program of study involving the newly invented atomic hydrogen maser frequency standard. He managed the maser R&D at Varian and continued to do so when Hewlett-Packard acquired the Beverly group. In 1969 he was appointed Physicist at the Smithsonian Astrophysical Observatory, Cambridge, Mass., and Research Associate at the Harvard College Observatory, Cambridge, where he is continuing research on the hydrogen maser and the use of atomic clocks in the experimental study of gravitation and relativity.